Journal Name

ARTICLE

Self-assembled artificial viral capsid bearing coiled-coils at the surface

Seiya Fujita and Kazunori Matsuura*

In order to construct artificial viral capsids bearing complementary dimeric coiled-coils on the surface, β-annulus peptide bearing a coiled-coil forming sequence at the C-terminus (β-annulus-coiled-coil-B) was synthesized by a native chemical ligation of β-annulus-SBn peptide with Cys-containing coiled-coil-B peptide. Dynamic light scattering (DLS) measurements and transmission electron microscope (TEM) images revealed that the β-annulus-coiled-coil-B peptide self-assembled into spherical structures of about 50 nm in 10 mM Tris-HCl buffer. Circular dichroism (CD) spectra indicated formation of the complementary coiled-coil structure on the spherical assemblies. Addition of 0.25 equivalent of complementary coiled-coil-A peptide to the β-annulus-coiled-coil-B peptide showed the formation of spherical assemblies of 46 ± 14 nm with grains of 5 nm at the surface, whereas addition of 1 equivalent of complementary coiled-coil-A peptide generated fibrous assemblies.

Introduction

Supramolecules constructed by self-assembly of rationally designed peptides and proteins have attracted much attention because of their potential to achieve non-natural functions. Rationally designed coiled-coil α-helices and β-sheets, which are typical structural motifs of proteins, have been employed as building blocks of various artificial supramolecules.[1] Coiled-coil is formed from two or more α-helices due to hydrophobic interactions and electrostatic interactions, of which the aggregation number can be regulated by replacement of hydrophobic amino acids.[2] To date, coiled-coil assemblies possessing various morphologies such as fibers,[3] tubes,[4] polyhedrons,[5] capsules,[6] and fractal structure[7] have been constructed from designed coiled-coil peptides.[8] Virus-like aggregates have also been constructed from coiled-coil motif. For example, Robinson et al. developed an antigen-displaying vesicle based on coiled-coil formation.[9] Ryadnov et al. reported virus-like aggregates consisting of RNA encapsulated in spherical coiled-coil assembly.[10]

Viruses are natural supramolecular assemblies with discrete size, consisting of genomic nucleic acids encapsulated in an outer protein shell known as capsid protein. Most spherical viral capsids are self-assembled from multiples of 60 proteins, which have regular icosahedral symmetry.[11] Recently, the discrete nanospace of viral capsids has attracted much attention as a nanocarrier and nanoreactor.[12] For example, Douglas et al. reported synthesis of iron oxide nanoparticles in the interior of cowpea chlorotic mottle virus (CCMV).[13] Cornelissen et al. encapsulated horse radish peroxidase

and green fluorescence protein (GFP) into the recombinant CCMV capsid.[14] The regular surface of viral capsids is also useful as a scaffold for the display of functional molecules such as carbohydrates,[15] proteins,[16] DNA,[17] quantum dots[18], and gold nanoparticles.[19]

Some natural viruses such as adenovirus and influenza virus have protein spikes on the surface. It is known that the spikes on the viral capsid increase cell-surface recognition and infectivity owing to the increased surface area. For example, influenza virus has trimer coiled-coil spikes known as hemagglutinin, of which three binding sites at the top recognize α2,3- or α2,6-sialyl lactose moiety of gangliosides on the host cell surface at infection.[20] Adenovirus has spikes of triple β-spiral structure with each penton base of the capsid that attach to the host cell via the receptor on the host cell surface.[21] Recently, Yamashita et al. constructed an artificial ball-and-spike protein supramolecule through the self-assembly of a fusion protein consisting of Dps protein from the bacterium Listeria innocua (LisDps) and cell punctuating needles (gp5C) of the T4 bacteriophage.[22]

We have developed an artificial viral capsid self-assembled from a 24-mer β-annulus peptide fragment (INHVGGTGGAIM APVAVTRQLVGS) which participates in the formation of the dodecahedral internal skeleton of tomato bushy stunt virus.[23] The pH dependence of the ζ-potentials of artificial viral capsid indicates that the C-terminus is directed to the surface, whereas the N-terminus is directed to the interior.[24] The artificial viral capsid can encapsulate anionic dyes, DNA,[24] and CdTe quantum dots[25] in the cationic interior. Using the N-terminus modification, His-tagged GFP[26] and fluorescent ZnO nanoparticles[27] were also encapsulated into the artificial viral capsid. The C-terminus modification allowed decoration of the

Department of chemistry and Biotechnology, Graduate School of Engineering, Tottori University, Tottori, 680-8552, Japan. Email: ma2ra-k@chem.tottori-u.ac.jp
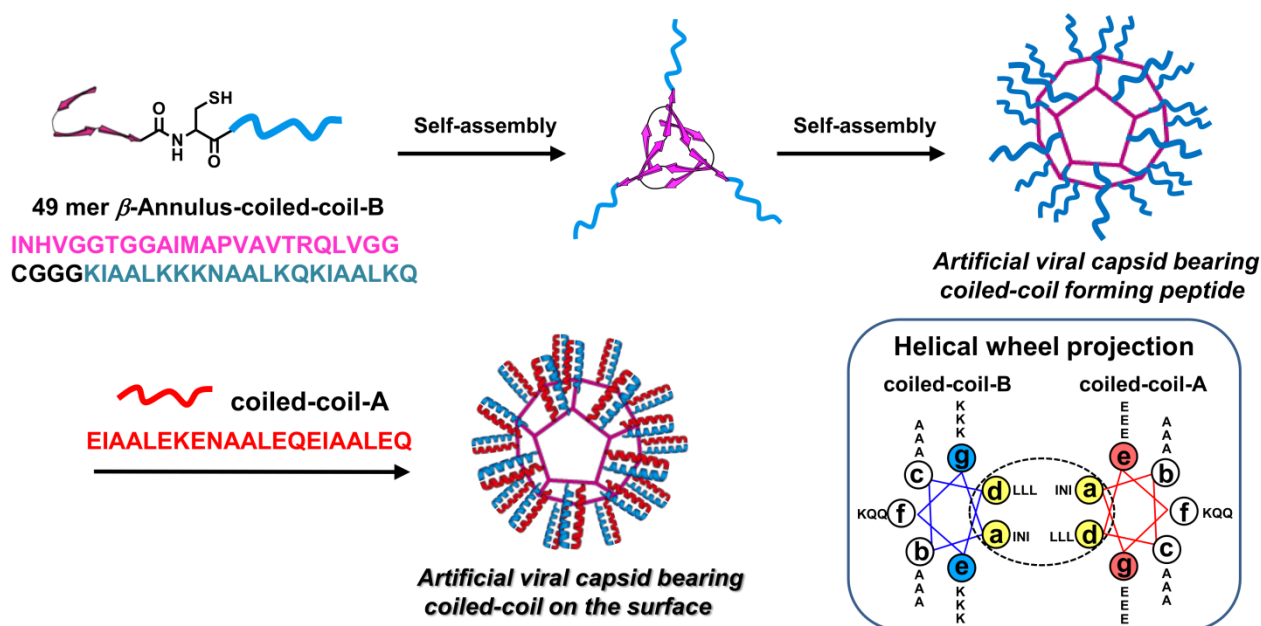
Figure 1. Schematic illustration of construction of artificial viral capsid bearing coiled-coils on the surface.

artificial viral capsid surface with gold nanoparticles[28] and DNA[29].

In this study, we describe the creation of an artificial viral capsid bearing coiled-coil structures on the surface, mimicking natural viruses bearing spikes (Figure 1). The hetero-dimeric coiled-coil forming sequence was designed using the methods described in Woolfson.[6] β-Annulus peptide bearing the coiled-coil forming sequence at the C-terminus was synthesized by native chemical ligation (NCL). Addition of complementary coiled-coil-A peptide to the artificial viral capsid self-assembled from β-annulus-coiled-coil-B peptide generated capsids with coiled-coil spikes on the surface.

Results and discussion

In general, it is difficult to synthesize peptides comprising approximately 50 residues, in high yield, using standard solid phase peptide synthesis (SPPS). Therefore, we synthesized the 49-mer β-annulus-coiled-coil-B peptide by the native chemical ligation (NCL) method,[30] in which peptides bearing unprotected cysteine residues at the N-terminus are ligated with C-terminus thioesterified peptide at neutral pH via S-N acyl shift. Dawson developed NCL using peptides activated with an N-acylbenzimidazolinone (Nbz) group at the C-terminus that can be synthesized by Fmoc-SPPS.[31] Recently, peptide syntheses by Dawson's NCL method have been reported[32] due to its advantages such as generation of activated peptide-esters by Fmoc solid phase synthesis without isolation of the protected peptide, and the ability to thioesterify the obtained peptide-Nbz in ligation buffer. Therefore, we synthesized β-annulus-coiled-coil-B peptide by NCL using the β-annulus-Nbz peptide, which can be synthesized with Fmoc-SPPS. Figure 2 shows the synthetic scheme of the β-annulus-coiled-coil-B peptide. β-Annulus-Nbz peptide (INHVGGTGGAIMAPVAVTRQLVGG-
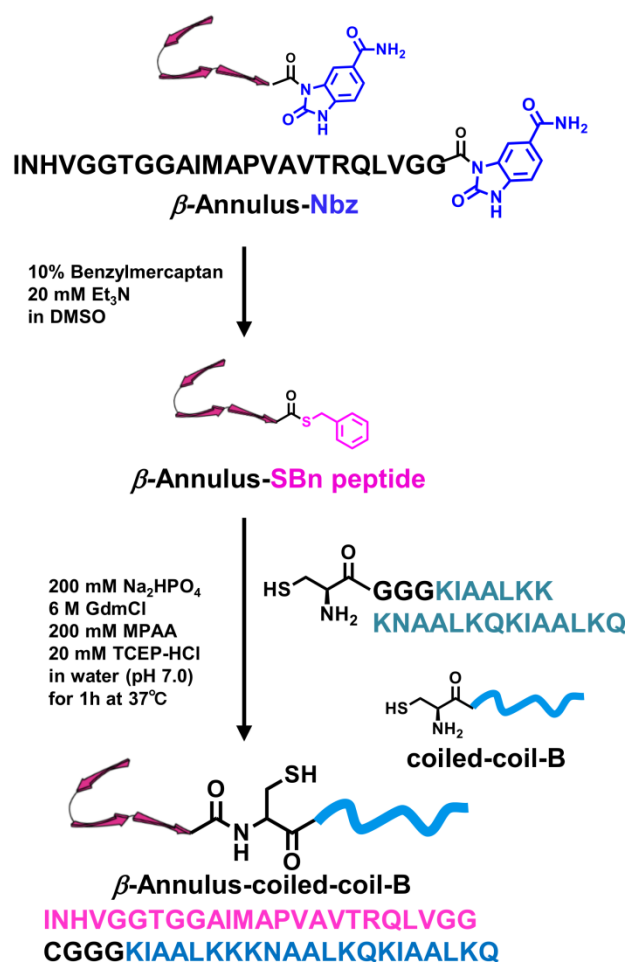

Figure 2. Synthesis of β-annulus-coiled-coil-B peptide by native chemical ligation.

Nbz) was synthesized at 0.25 mmol scale on commercially available Dawson Dbz AM resin. The amino group of the resin was protected by allyloxycarbonate (Alloc) to prevent branching before loading the first amino acid.[33] After loading the amino acid, the Alloc group was deprotected with $PhSiH_3$ and $Pd(PPh_3)_4$ and the resin was treated with *p*-nitrophenylchloroformate to convert the Nbz group. β-Annulus-Nbz peptide was deprotected and cleaved from the resin by treatment with a cleavage cocktail trifluoroacetic acid (TFA):water:1,2-ethanedithiol:triisopropylsilane = 9.5:0.25:0.25:0.1. Coiled-coil-A peptide (EIAALEKENAALEQEIAALEQ) and coiled-coil-B peptide (CGGGKIAALKKKNAALKQKIAALK

Q) were synthesized on Fmoc-NH-SAL resin using Fmoc-based coupling reactions. The coiled-coil-B peptide has a GGG linker between the Cys and coiled-coil forming sequence to reduce steric hindrance in the NCL reaction and coiled-coil formation on the artificial viral capsid. All peptides were purified by reverse phase-HPLC and confirmed by MALDI-TOF-MS.

Although Dawson reported that NCL proceeded by mixing peptide-Nbz and the Cys-containing peptide,[34] the NCL reaction between the β-annulus-Nbz peptide and coiled-coil-B peptide minimally proceeded because the hydrolysis of β-

annulus-Nbz peptide occurred faster than thioesterification of the peptide at C-terminus by 4-mercaptobenzoic acid (MPAA). To avoid hydrolysis of the β-annulus-Nbz peptide,[35] we tried
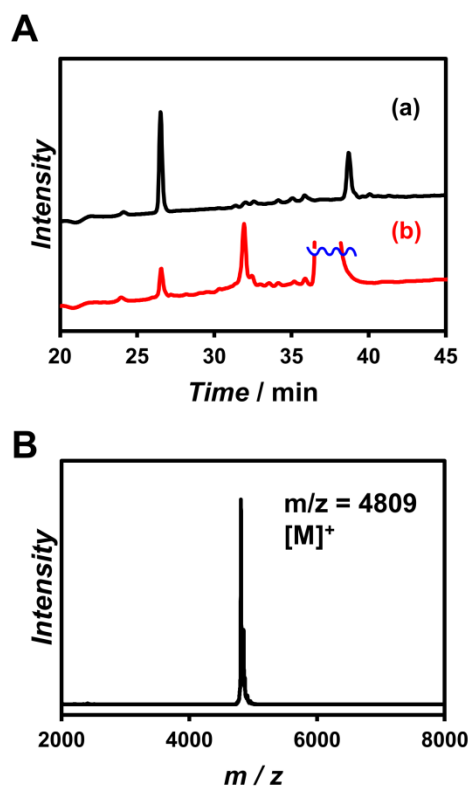

Figure 3. (A) Reverse-phase HPLC chromatograms of (a) mixture of β-annulus-SBn peptide and coiled-coil-B peptide, (b) NCL mixture (6M Gdn•HCl, 20 mM TCEP, 200 mM MPAA, 200 mM sodium phosphate, 1 mM β-annulus-SBn peptide , 1.5 mM coiled-coil-B peptide) reacted for 1h (B) MALDI-TOF-MS of the purified β-annulus-coiled-coil-B peptide.
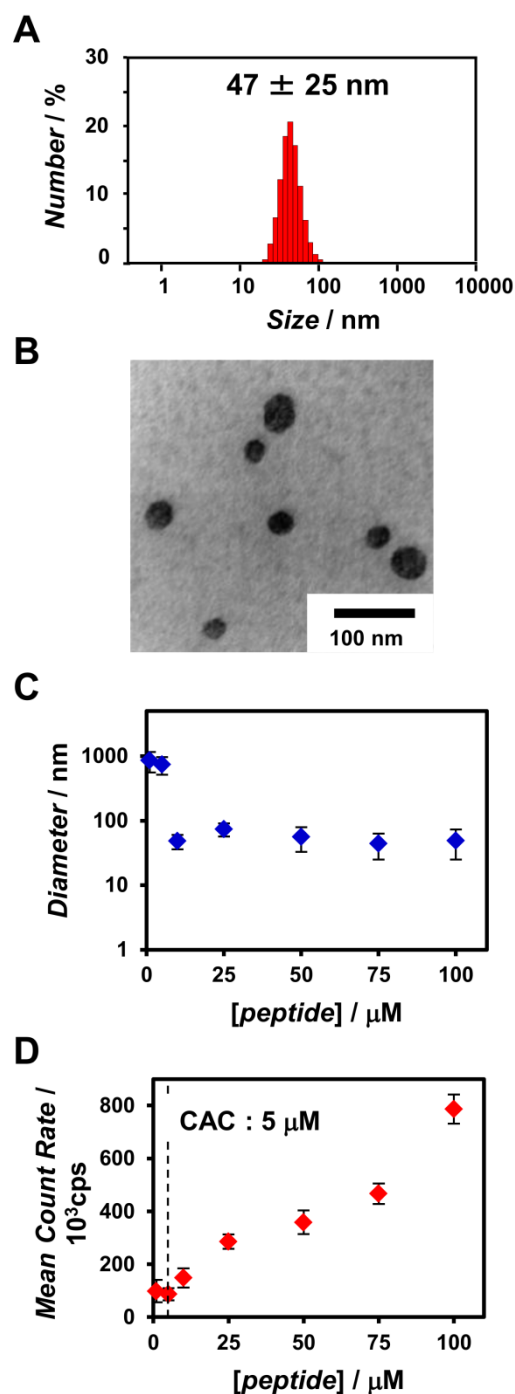

Figure 4. Size distribution obtained from Dynamic light scattering (DLS) (A) and transmission electron microscope (TEM) imaging (B) for an aqueous solution of β-annulus-coiled-coil-B peptide at 50 μM in 10 mM Tris-HCl buffer (pH 7.4) at 25°C. TEM samples were stained with sodium phosphotungstate. (C) Aggregate diameter as a function of peptide concentration. (D) Effect of peptide concentrations on the scattering intensity obtained from DLS in 10 mM Tris-HCl buffer (pH 7.4) at 25°C.

thioesterification of the peptide with thioester catalysis in DMSO, but thioester exchange in the NCL reaction did not occur. Thus, the β-annulus-Nbz peptide was converted into β-annulus-SBn peptide by addition of benzyl mercaptane and trimethylamine in DMSO. The obtained crude β-annulus-SBn peptide was used for synthesis of β-annulus-coiled-coil-B peptide by NCL without purification. The mixture of β-annulus-SBn peptide and 1.5 equivalent of coiled-coil-B peptide was incubated in NCL buffer for 1 h at 37°C. Reverse phase HPLC chart of the reaction mixture shows that two peaks assigned to β-annulus-SBn peptide at 38 min and coiled-coil B peptide at 27 min disappeared and a new peak appeared (Figure 3A). The new peak was confirmed as β-annulus-coiled-coil B peptide by MALDI-TOF-MS (Figure 3B).

The self-assembly behavior of the β-annulus-coiled-coil-B peptide in 10 mM Tris-HCl buffer (pH 7.4) was evaluated by dynamic light scattering (DLS) measurement and TEM observation. The average diameter obtained from DLS measurement of the peptide solution at 100 μM showed formation of assemblies with the size of 47 ± 25 nm (Figure 4A), which is comparable to the size of artificial viral capsid self-assembled from unmodified β-annulus peptide.[23] The TEM image of the peptide stained with sodium phosphotungstate showed the existence of spherical assemblies of 30-50 nm (Figure 4B), indicating formation of the artificial viral capsid. Figure 4C shows the peptide concentration dependence on the size distribution obtained from DLS. Similar assemblies of approximately 30–50 nm were formed at the concentration above 10 μM. In contrast, larger aggregates were observed at the concentration below 5 μM. This result might be caused by transient formation of large amorphous aggregates, because the dispersion of the autocorrelation functions at the concentration below 5 μM were large (Figure S1). The peptide concentration dependence on the 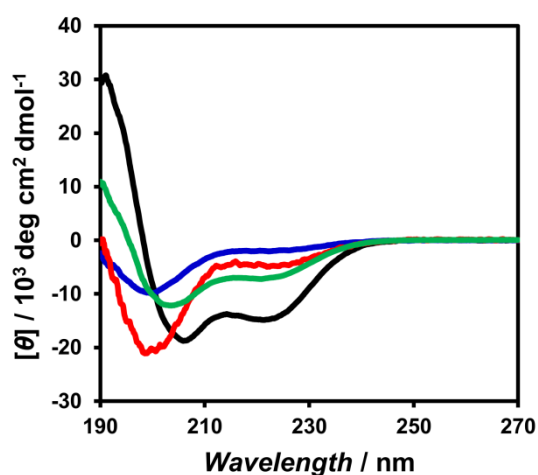scattering intensity indicates that the critical aggregation concentration (CAC) of the peptide in the buffer at 25°C is 5-10 μM. The obtained CAC suggests that the artificial viral capsid self-assembled from the β-annulus-coiled-coil-B peptide is more stable than the unmodified β-annulus peptide. This may be due to interactions among the coiled-coil-B peptides on the artificial viral capsid.

Formation of coiled-coils on the artificial viral capsid self-assembled from β-annulus-coiled-coil-B by the addition of complementary coiled-coil-A peptide was evaluated by circular dichroism (CD) spectrum (Figure 5). The CD spectrum of β-annulus-coiled-coil-B peptide showed the coexistence of random-coil and β-structures which is similar to the spectrum of unmodified β-annulus peptide. The coiled-coil-A peptide showed random coiling. In contrast, the CD spectrum of their mixture showed negative peaks at 222 nm and 208 nm which indicate formation

Figure 5. CD spectra of (red) coiled-coil-A peptide, (blue) β-annulus-coiled-coil-B peptide, (green) mixture of coiled-coil-A peptide and β-annulus-coiled-coil-B peptide, (black) mixture of coiled-coil-A peptide and coiled-coil-B peptide at [coiled-coil-A] = 12.5 μM, [coiled-coil-B] = [β-annulus-coiled-coil-B] = 50 μM in 10 mM Tris-HCl buffer (pH 7.4) at 25°C.
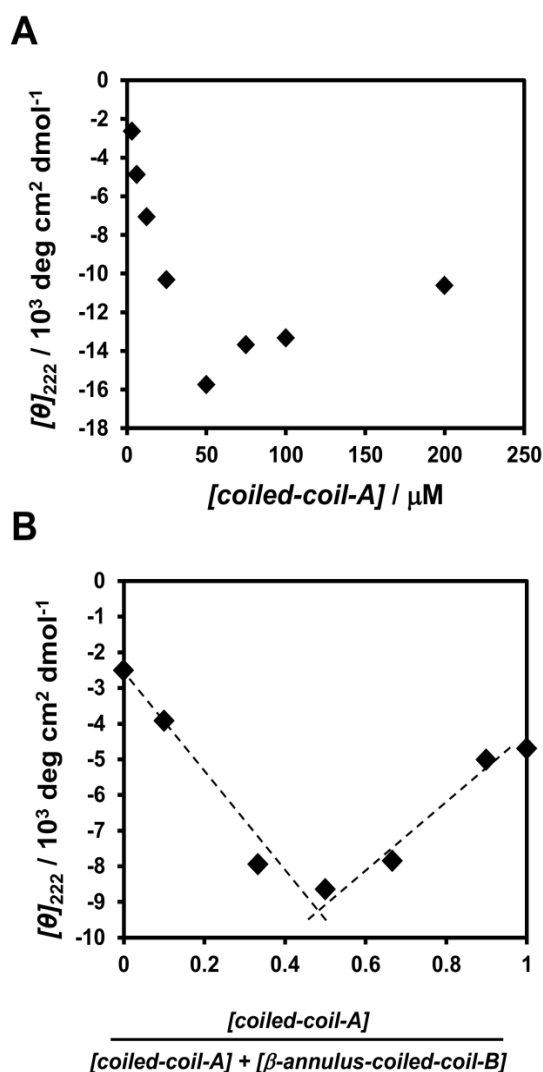

Figure 6. (A) The concentration dependence of coiled-coil-A peptide on the molar ellipticity at 222 nm of mixture of β-annulus-coiled-coil-B peptide (50 μM) and coiled-coil-A peptide. (B) The Job's plot obtained from the molar ellipticity at 222 nm of mixture of β-annulus-coiled-coil-B peptide and coiled-coil-A peptide.
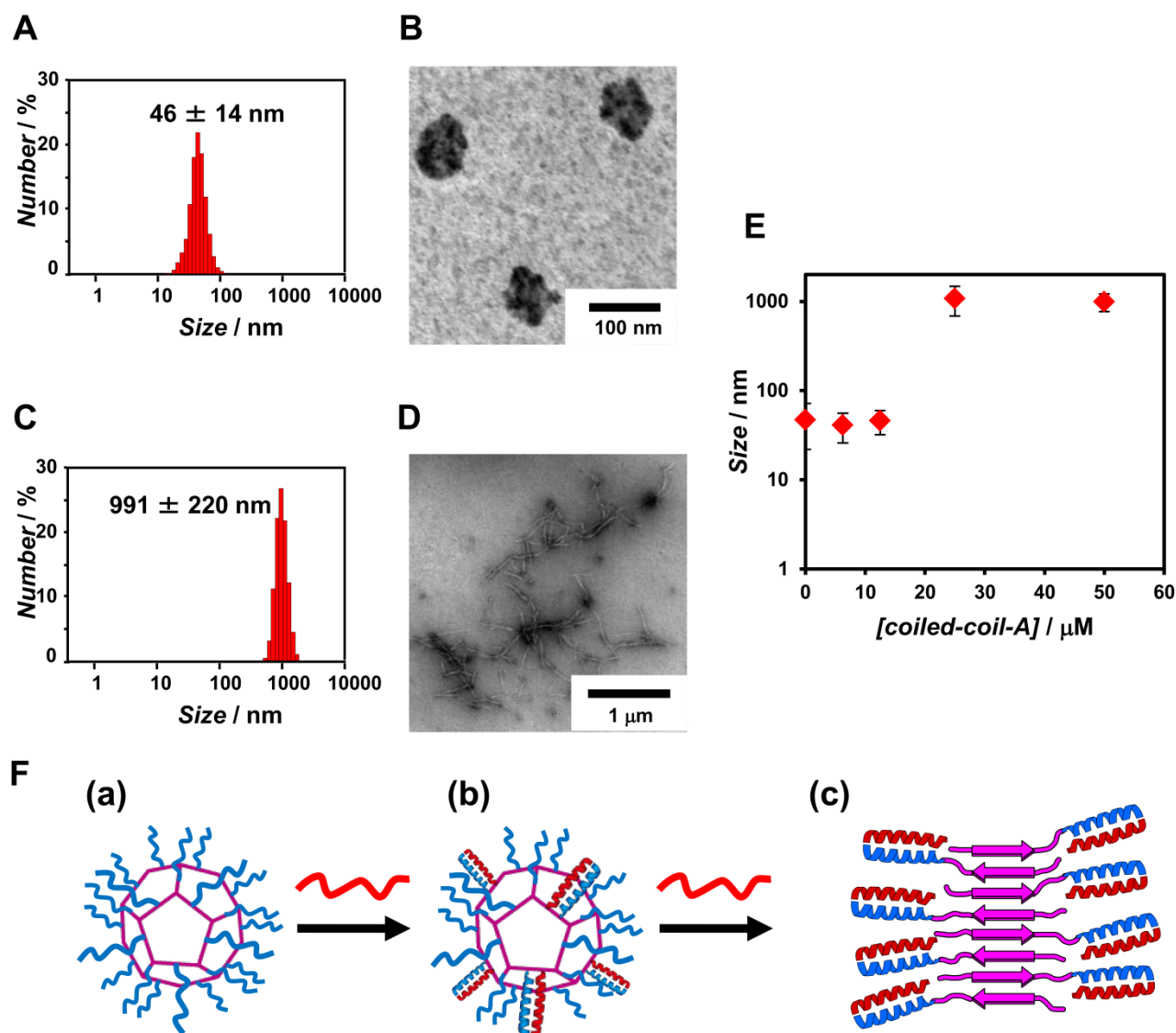
Figure 7. (A, B) Size distribution obtained from DLS (A) and TEM imaging (B) of the mixture of β-annulus-coiled-coil-B peptide (50 μM) and coiled-coil-A peptide at 12.5 μM in 10 mM Tris-HCl buffer (pH 7.4) at 25°C. (C, D) Size distribution obtained from DLS (C) and TEM image (D) of the mixture of β-annulus-coiled-coil-B peptide (50 μM) and coiled-coil-A peptide at 50 μM in 10 mM Tris-HCl buffer (pH 7.4) at 25°C. TEM samples stained with sodium phosphotungstate. (E) Aggregate diameter as a function of coiled-coil-A peptide concentration with β-annulus-coiled-coil-B peptide (50 μM) in 10 mM Tris-HCl buffer (pH 7.4) at 25°C. (F) Illustration of the assembly of β-annulus-coiled-coil-B peptide (50 μM) and coiled-coil-A peptide at the concentration of coiled-coil-A at 0 μM (a), 12.5 μM (b), and 50 μM (c).

of α-helix coiled-coil. Molar ellipticity of this mixture was lower than that of the mixture of coiled-coil-B and coiled-coil-A at the same concentration, suggesting formation of coiled-coils only at the coiled-coil-B sequence on the β-annulus-coiled-coil-B peptide. Green curve in Figure 5 was apparently smaller than black curve, because molar ellipticity of the CD spectrum was divided by the residue molar concentration. A difference spectrum subtracting β-annulus peptide from 4:1 mixture of β-annulus-coiled-coil-B peptide and coiled-coil-A peptide before dividing by the residue molar concentration showed the formation of about 80% coiled coil (Figure S3). Addition of coiled-coil-A peptide to 50 μM β-annulus-coiled-

coil-B peptide decreased the molar ellipticity at 222 nm until the concentration of coiled-coil-A of 50 μM (Figure 6A). In contrast, the molar ellipticity at 222 nm increased at coiled-coil-A concentrations above 50 μM. These results suggest that α-helix content increased at the concentration of 50 μM and less, whereas free coiled-coil-A peptide increased at the concentration of coiled-coil-A above 50 μM. The Job's plot of the molar ellipticity at 222 nm of the mixture of β-annulus-coiled-coil-B peptide and coiled-coil-A peptide indicated that the stoichiometric ratio of coiled-coil formation is 1:1 (figure 6B). Formation of assembly of β-annulus-coiled-coil-B peptide in the presence of coiled-coil-A peptide was evaluated using

DLS measurements and TEM observations. The size distribution obtained from DLS of the 4:1 mixture showed formation of assemblies with the size of 46 ± 14 nm (Figure 7A), which is comparable to the size of artificial viral capsid self-assembled from β-annulus-coiled-coil-B peptide alone (Figure 4A). In the TEM image of the 4:1 mixture, spherical assemblies with the size of 60 nm bearing grains of about 5 nm on the surface were abundantly observed (Figure 7B). In contrast, the TEM image of the 1:1 mixture indicated formation of fibrous assemblies with the length of about 1 μm (Figure 7D) which is supported by size distribution obtained from DLS measurement (Figure 7C). The size distribution of the mixtures is comparable to that of the artificial viral capsid at the concentrations of 12.5 μM and less, whereas larger assemblies formed with a size of about 1 μm at concentrations above 25 μM (Figure 7E). These results indicate that coiled-coil structures formed on the artificial viral capsid at the concentrations of coiled-coil-A of 12.5 μM and less, whereas fibrous assemblies formed at concentrations above 25 μM. The mechanism of fiber formation in the 1:1 mixture was examined whether the fiber consisted of β-sheet by using Thioflavin T, which is known that the fluorescence intensity increase by binding to amyloid fibril consisting of β-sheet. The fluorescence intensity of Thioflavin T did not increase in 4:1 mixture of β-annulus-coiled-coil-B peptide and coiled-coil-A peptide (Figure S4 blue), whereas the fluorescence intensity increased in the 1:1 mixture (Figure S4 green), indicating the formation of β-sheet fiber. It is possible that coiled-coils could not form on the artificial viral capsid because the C-terminus side of β-annulus-coiled-coil-B peptide crowded the artificial viral capsid at coiled-coil-A concentrations above 25 μM. Therefore, it is likely that the 1:1 mixture formed β-sheet fibrous assemblies by disrupting capsid structure (Figure 7F).

Conclusions

We synthesized a 49-mer β-annulus peptide bearing coiled-coil forming peptide at the C-terminus via the native chemical ligation method. The peptide self-assembled into an artificial viral capsid with the size of approximately 50 nm in Tris-HCl buffer. CD spectra showed the formation of coiled-coils with the addition of complementary coiled-coil-A peptide to the artificial viral capsid. DLS measurements and TEM observations of the mixture indicated the formation of an artificial viral capsid with grains on the surface. The dimeric coiled-coil structure on the surface of the artificial viral capsid is a promising platform to present various functional molecules such as receptor proteins to facilitate cellular uptake.

Experimental

General

Reagents were obtained from a commercial source and used without further purification. Reversed-phase HPLC was performed at ambient temperature with a Simadzu LC-6AD liquid chromatograph equipped with a UV/Vis detector (220 nm, Shimadzu SPD-20A) using GL Science Inertsil ODS-3

C18 (4.6 × 250 mm and 20 × 250 mm). MALDI-TOF mass spectra were obtained on an Autoflex II (Bruker Daltonics) spectrometer under the linear/positive mode with α-cyano-4-hydroxycinnamic acid (α-CHCA) as matrix.

Syntheses of peptides

Coiled-coil-B peptide: The peptide H-Cys(Trt)-Gly-Gly-Gly-Lys(Boc)-Ile-Ala-Ala-Leu-Lys(Boc)-Lys(Boc)- Lys(Boc)-Asn(Trt)-Ala-Ala--Leu-Lys(Boc)-Gln(Trt)-Lys(Boc)-Ile-Ala-Ala--Leu-Lys(Boc)-Gln(Trt)-resin was synthesized on Fmoc-NH-SAL Resin (Watanabe Chemical Ind. Ltd., 0.21 mmol/g) using Fmoc-based coupling reactions (4 equivalent of Fmoc amino acids). Solutions of (1-cyano-2-ethoxy-2-oxoethylidenaminooxy) dimethylamino-morpholino-carbenium hexafluorophosphate (COMU) and diisopropylamine in N-methylpyrrolidone (NMP) were used as coupling reagents. 20% Piperidine in N,N-dimethylformamide (DMF) was used for Fmoc deprotection. Progression of coupling reaction and Fmoc deprotection was confirmed by TNBS and chloranil test kit (Tokyo Chemical Industry Co., Ltd.). The peptidyl resin was washed with NMP. The peptide was deprotected and cleaved from the resin by treatment with a mixture of TFA:water:1,2-ethanedithiol:triisopropylsilane = 9.5:0.25:0.25:0.1 at room temperature for 3 h. The reaction mixture was filtered to remove the resin and the filtrate was concentrated under vacuum. The peptide was precipitated by adding methyl *tert*-butyl ether (MTBE) to the residue and the supernatant was decanted. After repeating the washing with MTBE thrice, the precipitated peptide was dried in vacuo. The crude product was purified by reverse-phase HPLC (RP-HPLC, Inertsil ODS3 C18) eluting with a linear gradient of CH_3CN/water containing 0.1% TFA (85/15 to 25/75 over 100 min). The fraction containing the desired peptide was lyophilized to give 7 mg of a flocculent solid (5.9% yield). MALDI-TOF MS (matrix: α-CHCA): m/z = 2552 [M]$^+$.

Coiled-coil-A peptide (EIAALEKENAALEQEIAALEQ): The peptide was synthesized by almost the same procedure described above. After loading the amino acid, the peptidyl resin was added to the mixture of 3 equivalent of acetic anhydride and 4.5 equivalent of DIPEA in DMF to protect the amine of N-terminus by acetyl group. The isolated yield was 6.8%. MALDI-TOF-MS (matrix : α-CHCA): m/z = 2325 [M]$^+$.

β-Annulus-Nbz peptide: The β-annulus peptide functionalized at the C-terminus with an N-acyl-benzimid-azolinone (INHVGGTGGAIMAPVAVTRQLVGG-Nbz) was synthesized at 0.25 mmol scale on commercially available Dawson Dbz AM resin (Novabiochem®, San Diego, CA, USA). The amino group of the resin was protected by allyloxycarbonate (Alloc) with a mixture of 7 equivalent of Allylchloroformate and 1 equivalent of DIPEA at room temperature for 24 h. Loading of amino acid and deprotection of the Fmoc-group were done by almost same procedure described above. After loading of the amino acid, deprotection of the Alloc group was used as a mixture of 20 equivalent of PhSiH$_3$ and 0.35 equivalent of Pd(PPh$_3$)$_4$ in DCM. Then, the resin was treated with 5 equivalent of *p*-nitrophenylchloroformate in DCM followed by 0.5 M DIPEA in DMF to converted Nbz group. The peptide was deprotected and cleaved from the resin by treatment with

cleavage cocktail for 3 h. The crude yield was 30%. MALDI-TOF-MS (matrix:α-CHCA): m/z = 2435 [M]$^+$.

Preparation of β-annulus-SBn peptide

Crude β-annulus-Nbz peptide powder was added to a mixture of 10% benzyl mercaptane and 20 mM triethylamine in DMSO to convert to benzylthioesterified β-annulus peptide at the C-terminus. After the solution was incubated at 37°C for 15 min, the peptide was precipitated by adding ethyl acetate to the reaction mixture and the supernatant was decanted. After repeating the washing with ethyl acetate thrice, the precipitated peptide was dried under vacuum. The precipitated peptide was used for native chemical ligation without further purification. The yield was 66%. MALDI-TOF MS (matrix:α-CHCA): m/z = 2381 [M]$^+$.

Native Chemical Ligation

NCL buffer (pH 7.0) was prepared by dissolving 6M guanidinium hydrochloride (Gdn•HCl), 20 mM triscarboxyethyl phosphine (TCEP), 200 mM 4-mercaptophenylacetic acid (MPAA), 200 mM sodium phosphate in water and degassed with N$_2$. The coiled-coil-B peptide bearing cysteine at N-terminus (0.75 μmol) and β-annulus-SBn peptide (0.5 μmol) were dissolved in NCL buffer and the mixture was incubated at 37°C for 1 h. The reaction mixture purified by reverse-phase HPLC (Inertsil ODS3 C18) eluting with a linear gradient of CH$_3$CN:water containing 0.1% TFA (80:20 to 60:40 over 100 min). The isolated yield was 42.7%. MALDI-TOF MS (matrix:α-CHCA): m/z = 4809[M]$^+$.

Dynamic light scattering (DLS) measurements

Stock solutions (1.0 mM) of peptide were dissolved in 10 mM Tris-HCl buffer without sonication or heating. Samples were prepared by diluting stock solutions with 10 mM Tris-HCl buffer and were incubated at 25°C for 1 h before measurements using a Zetasizer NanoZS (Malvern Instruments Ltd.) instrument with incident He-Ne laser (633 nm). The correlation time of scattered light intensity $G(\tau)$ was measured several times and the averaged data were fitted to equation (2), where B is a baseline, A is amplitude, q is scattering vector, τ is delay time, and D is the diffusion coefficient.

$$G(\tau) = B + A \exp(-2q^2 D\tau) \quad (2)$$

The hydrodynamic radius (R_H) of the scattering particles was calculated by the Stokes-Einstein equation (eq. 3), where η is solvent viscosity, k_B is Boltzmann's constant, and T denotes the absolute temperature.

$$R_H = \frac{k_B T}{6\pi\eta D} \quad (3)$$

Transmission electron microscopy (TEM)

An aliquot (5 μL) of DLS sample solutions was applied to a carbon coat grid (C-SMART Hydrophilic TEM gilds, ALLANCE Biosystems), left for 60 s, and removed. A drop of 2 wt% aqueous sodium phosphotungstate was placed on each of the grids. The sample-loaded carbon-coated grids were dried in vacuo. The carbon coat grids were subjected to TEM observation (JEOL JEM 1400 Plus) with acceleration voltage of 80 kV.

CD spectra

CD spectra were recorded at 25°C with a JASCO J-820 spectrophotometer using a 1-mm quartz cell. A series of mixtures containing β-annulus-coiled-coil-B peptide and coiled-coil-A peptide were prepared such that the sum of their total peptide concentration remained constant (50 μM), and the mixtures were incubated for 1 h before measurement. The mole fraction of coiled-coil-A peptide was varied from 0 to 1. The molar ellipticity at 222 nm was plotted against the molar fraction of the coiled-coil-A peptide to estimate the stoichiometry.

Acknowledgements

Notes and references

1　(a) K. Matsuurua, *RSC Adv.*, 2014, **4**, 2942-2953. (b) B. E. I. Ramakers, J. C. M. van Hest and D. Lowik, *Chem. Soc. Rev.*, 2014, **43**, 2743-2756. (c) E. D. Santis, M. G. Ryadnov, *Chem. Soc. Rev.* 2015, **44**, 8288-8300. (d) Q. Luo, C. X. Hou, Y. S. Bai, R. B. Wang and J. Q. Liu, *Chem. Rev.*, 2016, **116**, 13571-13632.

2　(a) J. M. Fletcher, A. L. Boyle, M. Bruning, G. J. Bartlett, T. L. Vincent, N. R. Zaccai, C. T. Armstrong, E. H. C. Bromley, P. J. Booth, R. L. Brady, A. R. Thomson and D. N. Woolfson, *ACS Synth. Biol.*, 2012, **1**, 240-250. (b) F. Thomas, A. L. Boyle, A. J. Burton, D. N. Woolfson, *J. Am. Chem. Soc.*, 2013, **135**, 5161-5166.

3　(a) S. A. Potekhin, T. N. Melnik, V. Popov, N. F. Lanina, A. A. Vazina, P. Rigler, A. S. Verdini, G. Corradin and A. V. Kajava, *Chem. Biol.*, 2001, **8**, 1025-1032. (b) N. L. Ogihara, G. Ghirlanda, J. W. Bryson, M. Gingery, W. F. DeGrado and D. Eisenberg, *Proc. Natl. Acad. Sci. U. S. A.*, 2001, **98**, 1404-1409. (c) M. Zhou, D. Bentley and I. Ghosh, *J. Am. Chem. Soc.*, 2004, **126**, 734-735. (d) Y. Zimenkov, S. N. Dublin, R. Ni, R. S. Tu, V. Breedveld, R. P. Apkarian and V. P. Conticello, *J. Am. Chem. Soc.*, 2006, **128**, 6770-6771. (e) T. H. Sharp, M. Bruning, J. Mantell, R. B. Sessions, A. R. Thomson, N. R. Zaccai, R. L. Brady, P. Verkade and D. N. Woolfson, *Proc. Natl. Acad. Sci. U. S. A.*, 2012, **109**, 13266-13271. (f) J. Hume, J. Sun, R. Jacquet, P. D. Renfrew, J. A. Martin, R. Bonneau, M. L. Gilchrist and J. K. Montclare, *Biomacromolecules*, 2014, **15**, 3503-3510.

4　(a) C. F. Xu, R. Liu, A. K. Mehta, R. C. Guerrero-Ferreira, E. R. Wright, S. Dunin-Horkawicz, K. Morris, L. C. Serpell, X. B. Zuo, J. S. Wall and V. P. Conticello, *J. Am. Chem. Soc.*, 2013, **135**, 15565-15578. (b) N. C. Burgess, T. H. Sharp, F. Thomas, C. W. Wood, A. R. Thomson, N. R. Zaccai, R. L. Brady, L. C. Serpell and D. N. Woolfson, *J. Am. Chem. Soc.*, 2015, **137**, 10554-10562. (c) F. Thomas, N. C. Burgess, A. R. Thomson, D. N. Woolfson, *Angew. Chem. Int. Ed.*, 2016, **55**, 987-991.

5　(a) H. Gradisar, S. Bozic, T. Doles, D. Vengust, I. Hafner-Bratkovic, A. Mertelj, B. Webb, A. Sali, S. Klavzar and R. Jerala, *Nat. Chem. Biol.*, 2013, **9**, 362-366. (b) N.

Kobayashi, K. Yanase, T. Sato, S. Unzai M. H. Hecht, R. Arai, *J. Am. Chem. Soc.* 2015, **137**, 11285-11293.

6   (a) J. M. Fletcher, R. L. Harniman, F. R. H. Barnes, A. L. Boyle, A. Collins, J. Mantell, T. H. Sharp, M. Antognozzi, P. J. Booth, N. Linden, M. J. Miles, R. B. Sessions, P. Verkade and D. N. Woolfson, *Science*, 2013, **340**, 595-599. (b) W. M. Park and J. A. Champion, *J. Am. Chem. Soc.*, 2014, **136**, 17906-17909.

7   A. Lomander, W. M. Hwang and S. G. Zhang, *Nano Lett.*, 2005, **5**, 1255-1260.

8   Y. Wu, J. H. Collier, *WIREs Nanomed. Nanotechnol.*, 2017, DOI: 10.1002/wnan.1424.

9   F. Boato, R. M. Thomas, A. Ghasparian, A. Freund-Renard, K. Moehle and J. A. Robinson, *Angew. Chem. Int. Ed.*, 2007, **46**, 9015-9018.

10   J. E. Noble, E. De Santis, J. Ravi, B. Lamarre, V. Castelletto, J. Mantell, S. Ray and M. G. Ryadnov, *J. Am. Chem. Soc.*, 2016, **138**, 12202–12210.

11   (a) L. Liljas, *Prog. Biophys. Molec. Biol.*, 1986, **48**, 1-36. (b) *Introduction to Protein Structure*, C. Branden, J. Tooze, Garland Publishing, NewYork, 1999

12   (a) C. Chen, E. S. Kwak, B. Stein, C. C. Kao and B. Dragnea, *J. Nanosci. Nanotech*, 2005, **5**, 2029-2033. (b) T. Douglas and M. Young, *Science*, 2006, **312**, 873-875. (c) C. Chen, M. C. Daniel, Z. T. Quinkert, M. De, B. Stein, V. D. Bowman, P. R. Chipman, V. M. Rotello, C. C. Kao and B. Dragnea, *Nano Lett.*, 2006, **6**, 611-615. (d) S. K. Dixit, N. L. Goicochea, M. C. Daniel, A. Murali, L. Bronstein, M. De, B. Stein, V. M. Rotello, C. C. Kao and B. Dragnea, *Nano Lett.*, 2006, **6**, 1993-1999. (e) X. L. Huang, L. M. Bronstein, J. Retrum, C. Dufort, I. Tsvetkova, S. Aniagyei, B. Stein, G. Stucky, B. McKenna, N. Remmes, D. Baxter, C. C. Kao and B. Dragnea, *Nano Lett.*, 2007, **7**, 2407-2416. (f) N. F. Steinmetz, T. Lin, G. P. Lomonossoff and J. E. Johnson, *Viruses Nanotechnol.*, 2009, **327**, 23-58.

13   T. Douglas, E. Strable, D. Willits, A. Aitouchen, M. Libera and M. Young, *Adv. Mater.*, 2002, **14**, 415-418.

14   (a) M. Comellas-Aragonès, H. Engelkamp, V. I. Claessen, N. A. J. M. Sommerdijk, A. E. Rowan, P. C. M. Christianen, J. C. Maan, B. J. M. Verduin, J. J. L. M. Cornelissen, and R. J. M. Nolte, *Nature Nanotech.*, 2007, **2**, 635-639. (b) I. J. Minten, L. J. A. Hendriks, R. J. M. Nolte, and J. J. L. M. Cornelissen, *J. Am. Chem. Soc.*, 2009, **131**, 17771-17773.

15   K. S. Raja, Q. Wang, M. G. Finn, *ChemBioChem*, 2003, **4**, 1348-1351.

16   B. Schwarz, P. Madden, J. Avera, B. Gordon, K. Larson, H. M. Miettinen, M. Uchida, B. LaFrance, G. Basu, A. Rynda-Apple, T. Douglas, *ACS Nano*, 2015, **9**, 9134-9147.

17   (a) E. Strable, J. E. Johnson, M. G. Finn. *Nano Lett.* 2004, **4**, 1385-1389. (b) G. J. Tong, S. C. Hsiao, Z. M. Carrico, M. B. Francis, *J. Am. Chem. Soc.* 2009, **131**, 11174-11178.

18   F. Li, D. Gao, X. M. Zhai, Y. H. Chen, T. Fu, D. M. Wu, Z. P. Zhang, X. E. Zhang and Q. B. Wang, *Angew. Chem. Int. Ed.*, 2011, **50**, 4202-4205.

19   (a) A. S. Blum, C. M. Soto, C. D. Wilson, J. D. Cole, M. Kim, B. Gnade, A. Chatterji, W. F. Ochoa, T. W. Lin, J. E. Johnson and B. R. Ratna, *Nano Lett.*, 2004, **4**, 867-870. (b) A. S. Blum, C. M. Soto, C. D. Wilson, T. L. Brower, S. K. Pollack, T. L. Schull, A. Chatterji, T. W. Lin, J. E. Johnson, C. Amsinck, P. Franzon, R. Shashidhar and B. R. Ratna, *Small*, 2005, **1**, 702-706.

20   (a) W. Weis, J. H. Brown, S. Cusack, J. C. Paulson, J. J. Skehel and D. C. Wiley, *Nature*, 1988, **333**, 426-431. (b) S. J. Gamblin, L. F. Haire, R. J. Russell, D. J. Stevens, B. Xiao, Y. Ha, N. Vasisht, D. A. Steinhauer, R. S. Daniels, A. Elliot, D. C. Wiley and J. J. Skehel, *Science*, 2004, **303**, 1838-

1842. (c) B. Szewczyk, K. Bienkowska-Szewczyk and E. Krol, *Acta Biochim. Pol.*, 2014, **61**, 397-401.

21   (a) M. J. van Raaij, A. Mitraki, G. Lavigne and S. Cusack, *Nature*, 1999, **401**, 935-938. (b) G. R. Nemerow, P. L. Stewart and V. S. Reddy, *Current Opinion in Virology*, 2012, **2**, 115-121.

22   K. Sugimoto, S. Kanamaru, K. Iwasaki, F. Arisaka and I. Yamashita, *Angew. Chem. Int. Ed.*, 2006, **45**, 2725-2728.

23   (a) K. Matsuura, K. Watanabe, T. Matsuzaki, K. Sakurai and N. Kimizuka, *Angew. Chem. Int. Ed.*, 2010, **49**, 9662-9665. (b)K. Matsuura, *Polymer J.*, 2012, **44**, 469-474.

24   K. Matsuura, K. Watanabe, Y. Matsushita and N. Kimizuka, *Polymer J.*, 2013, **45**, 529-534.

25   S. Fujita and K. Matsuura, *Chem. Lett.*, 2016, **45**, 922-924.

26   K. Matsuura, T. Nakamura, K. Watanabe, T. Noguchi, K. Minamihata, N. Kamiya and N. Kimizuka, *Org. Biomol. Chem.*, 2016, **14**, 7869-7874.

27   (a) S. Fujita and K. Matsuura, *Nanomaterials*, 2014, **4**, 778-791.

28   K. Matsuura, G. Ueno and S. Fujita, *Polymer J.*, 2015, **47**, 146-151.

29   Y. Nakamura, S. Yamada, S. Nishikawa, K. Matsuura, *J. Pept. Sci.*, 2017 [DOI: 10.1002/psc.2967]

30   P. E. Dawson, T. W. Muir, I. Clarklewis and S. B. H. Kent, *Science*, 1994, **266**, 776-779.

31   J. B. Blanco-Canosa and P. E. Dawson, *Angew. Chem. Int. Ed.*, 2008, **47**, 6851-6855.

32   (a)S. Batjargal, Y. Huang, Y. X. J. Wang and E. J. Petersson, *J. Pept. Sci.*, 2014, **20**, 87-91. (b) R. Okamoto, K. Mandal, M. Ling, A. D. Luster, Y. Kajihara and S. B. H. Kent, *Angew. Chem. Int. Ed.*, 2014, **53**, 5188-5193. (c) S. Khan, S. Sur, P. Y. W. Dankers, R. M. P. da Silva, J. Boekhoven, T. A. Poor and S. I. Stupp, *Bioconj. Chem.*, 2014, **25**, 707-717.

33   S. K. Mahto, C. J. Howard, J. C. Shimko and J. J. Ottesen, *ChemBioChem*, 2011, **12**, 2488-2494.

34   M. Dittmann, J. Sauermann, R. Seidel, W. Zimmermann and M. Engelhard, *J. Pept. Sci.*, 2010, **16**, 558-562.